Non-adiabatic transitions in a two-state exponential potential model

2000 J. Phys. A: Math. Gen. 33 3361

(http://iopscience.iop.org/0305-4470/33/16/322)

J. Phys. A: Math. Gen. **33** (2000) 3361–3384. Printed in the UK PII: S0305-4470(00)10153-2

Non-adiabatic transitions in a two-state exponential potential model

Lukáš Pichl†, Vladimir I Osherov‡§ and Hiroki Nakamura†‡

† Department of Functional Molecular Science, School of Mathematical and Physical Science, Graduate University for Advanced Studies, Myodaiji, Okazaki 444-8585, Japan
‡ Division of Theoretical Studies, Institute for Molecular Science, Myodaiji, Okazaki 444-8585, Japan
§ Institute of Chemical Physics, Russian Academy of Sciences, Chernogolovka, Moscow 142432, Russia

Received 6 December 1999

Abstract. A general two-state exponential potential model is investigated and the corresponding two-channel scattering problem is solved by means of semiclassical theory. The analytical expression for the non-adiabatic transition matrix yields a unified expression in the repulsive and previously studied attractive case. The final formulae are expressed in terms of model-independent quantities, i.e. the contour integrals of adiabatic local momenta. Oscillations of the overall transition probability below the crossing of diabatic potentials are observed in the case of strong coupling. The theory is demonstrated to work very well even at energies lower than the diabatic crossing region. Based on our results the unified theory of non-adiabatic transitions, covering the Landau–Zener–Stueckelberg and Rozen–Zener–Demkov models in such an energy range, is possible.

1. Introduction

It is well known that non-adiabatic transitions play an important role in various fields of physics, chemistry and biology [1–3]. Treating them with mathematical rigour has been a problem challenged for many decades so that a full account of the progress achieved cannot be given here (see, e.g., [4–7] and references therein).

The most fundamental models of non-adiabatic transitions are classified into the Landau–Zener–Stueckelberg-type (LZS) curve crossing and the Rozen–Zener–Demkov-type (RZD) non-crossing problem. Over the last several years, the LZS problems have been solved completely [6–8], and an efficient and accurate theory has been successfully developed even for multi-channel curve-crossing problems [9, 10]. On the other hand, the exact analytical solution of the RZD model was obtained recently by Osherov and Voronin [11]. In addition, the exact quantum mechanical solution was found for some special exponential potential models [12, 13]. This remarkable progress encourages our efforts to formulate a unified theory that would hopefully cover the above-mentioned cases and to give a general formula for the non-adiabatic transition matrix in terms of integrals along the adiabatic potentials.

Here we are concerned with such an exponential model that the diabatic potentials and coupling are given by the same exponential function (see equation (2) below). The easier attractive case was examined in detail previously [14], and thus in this work the main attention is paid to the semiclassical treatment of the repulsive case. The purpose is to give a derivation of precise formulae of basic parameters which should be used in Nikitin's model [1] and which

0305-4470/00/163361+24$30.00

has not been known so far. Furthermore, it is confirmed that the non-adiabatic transition matrix in the exponential model covers both the Landau–Zener (LZ) and the Rozen–Zener-type (RZ) matrices as limiting cases. Based on these results the unification of LZ and RZ can be made and will be reported.

This paper is organized as follows. In section 2 we define the exponential model and review the treatment of the attractive case. In section 3 the total wavefunction for the repulsive model is obtained by the Wentzel–Kramer–Brillouin-type (WKB) semiclassical methods. In section 4 the scattering and non-adiabatic transition matrices are given and the validity of the double-passage formula is demonstrated. The final formulae are expressed in terms of the model-independent parameters, and are applicable to general potentials. Its accuracy is demonstrated in section 5 by using various numerical examples. We conclude with remarks on the future research in section 6. The appendix contains the most mathematical parts of this paper.

2. Preliminaries

We solve the coupled Schrödinger equations

$$\left[-\frac{\hbar^2}{2M}\frac{\mathrm{d}^2}{\mathrm{d}x^2}+\mathbf{V}(x)\right]\psi(x)=E\psi(x) \tag{1}$$

with

$$\psi=\begin{pmatrix}\psi_1(x)\\ \psi_2(x)\end{pmatrix}$$

and

$$\mathbf{V}(x)=\begin{pmatrix}U_1-V_1\exp(-\alpha x) & V\exp(-\alpha x)\\ V\exp(-\alpha x) & U_2-V_2\exp(-\alpha x)\end{pmatrix}. \tag{2}$$

In dimensionless units $[E]=\hbar^2\alpha^2(2M)^{-1}$ and $[x]=\alpha^{-1}$, the above equations have the form

$$-\psi_1''(x)+(U_1-V_1\exp(-x)-E)\,\psi_1(x)+V\exp(-x)\psi_2(x)=0 \tag{3}$$

and

$$-\psi_2''(x)+(U_2-V_2\exp(-x)-E)\,\psi_2(x)+V\exp(-x)\psi_1(x)=0.$$

Without loss of generality we choose $U_1>U_2$. In both attractive ($V_i>0$) and repulsive ($V_i<0$) cases we assume that $V_1V_2>V^2$ in order to avoid the case of three asymptotically open channels. In the adiabatic representation the coupling is localized and the diagonal adiabatic potentials are given by

$$u_{1,2}^{(a)}(x)=\tfrac{1}{2}(V_{11}+V_{22})\pm\left[\left(\tfrac{1}{2}(V_{11}-V_{22})\right)^2+V_{12}^2\right]^{1/2} \tag{4}$$

where $V_{ij}(x)$ are the elements of the matrix $\mathbf{V}(x)$ in equation (2). The adiabatic wavefunctions $\phi_i(x)$ $(i=1,2)$ obey the transformation,

$$\begin{pmatrix}\phi_1(x)\\ \phi_2(x)\end{pmatrix}=\mathbf{R}(\theta(x))\begin{pmatrix}\psi_1(x)\\ \psi_2(x)\end{pmatrix} \tag{5}$$

where

$$\mathbf{R}(\theta)=\begin{pmatrix}\cos\theta & -\sin\theta\\ \sin\theta & \cos\theta\end{pmatrix}\qquad\text{with}\quad\theta(x)=\tfrac{1}{2}\arctan\left(\frac{2V_{12}(x)}{V_{22}(x)-V_{11}(x)}\right) \tag{6}$$

and $\theta \in [0,\ \pi/2]$. A new variable ρ defined by

$$\rho = 2\sqrt{|V|}\exp\left(-\tfrac{1}{2}x\right) \tag{7}$$

and the parameters

$$\mu \equiv 2\sqrt{E-U_2} \qquad \nu \equiv 2\sqrt{E-U_1} \qquad \text{and} \qquad \beta_i \equiv \frac{V_i}{|V|} \tag{8}$$

reduce the coupled differential equations (3) into the following form:

$$\left[\rho^2\frac{\mathrm{d}^2}{\mathrm{d}\rho^2} + \rho\frac{\mathrm{d}}{\mathrm{d}\rho} + \nu^2 + \beta_1\rho^2\right]\psi_1 = \rho^2\psi_2 \tag{9}$$

and

$$\left[\rho^2\frac{\mathrm{d}^2}{\mathrm{d}\rho^2} + \rho\frac{\mathrm{d}}{\mathrm{d}\rho} + \mu^2 + \beta_2\rho^2\right]\psi_2 = \rho^2\psi_1.$$

In order to decouple equation (9) we perform the modified Bessel transformation

$$\psi_i(\rho) = \int_C \mathrm{d}p\ pF_i(p)\ Z_a(\rho p) \tag{10}$$

where C is a certain contour in the complex p-plane. Z_a denotes any appropriate kind of Bessel function ($H^{(1,2)}_{\pm i\nu}$ here) [15], which satisfies

$$\left[z^2\frac{\mathrm{d}^2}{\mathrm{d}z^2} + z\frac{\mathrm{d}}{\mathrm{d}z}\right]Z_a(z) = -\left(z^2+\nu^2\right)Z_a(z). \tag{11}$$

We note that it is necessary to choose appropriate combinations of the Bessel function Z and the corresponding contour C in equation (10) in order (a) to satisfy the boundary conditions and (b) to fulfil the conditions imposed on the asymptotic behaviour of $F_j(p)$ by the Bessel transformation [14]. It suffices to use an appropriate kind of Bessel function for each independent solution.

Having substituted equation (10) into (9), we can decouple $F_2(p)$ from $F_1(p)$ as

$$F_2(p) = \mathrm{sgn}(V)\left(\beta_1 - p^2\right)F_1(p). \tag{12}$$

In the obtained exact differential equation for $F_1(p)$ we first cancel $F_1'(p)$ by substituting

$$f_1(p) \equiv \sqrt{p}\left(p^2-a_1\right)\left(p^2-a_2\right)F_1(p) \tag{13}$$

where

$$a_{1,2} = \tfrac{1}{2}(\beta_1+\beta_2) \mp \sqrt{[\tfrac{1}{2}\ (\beta_1-\beta_2)]^2+1}. \tag{14}$$

The meaning of $|a_iV|$ in equation (14) is nothing but a pre-exponential constant of the ith adiabatic potential in the classically forbidden region (see equations (4) and (8)). From now on, we use the semiclassical approximation throughout the text, and where it is mentioned explicitly, also the high-energy limit. The resulting differential equation for $f_1(p)$ is further reduced to the following semiclassical form (taking $\mu^2,\ \nu^2,\ \mu^2-\nu^2 \gg 1$, i.e. α small, M large):

$$\left[\frac{\mathrm{d}^2}{\mathrm{d}p^2} + P_0(p)\right]f_1(p) = 0 \tag{15}$$

where

$$P_0(p) \equiv \frac{\mu^2}{p^2}\frac{\left(p^2-c_1\right)\left(p^2-c_2\right)}{\left(p^2-a_1\right)\left(p^2-a_2\right)} \tag{16}$$

and the coefficients c_1 and c_2 are defined as

$$c_{1,2} = \frac{1}{2}\left(\beta_1+\beta_2\frac{\nu^2}{\mu^2}\right) \mp \sqrt{\left[\frac{1}{2}\left(\beta_1-\beta_2\frac{\nu^2}{\mu^2}\right)\right]^2+\frac{\nu^2}{\mu^2}}. \tag{17}$$

At high energies zeros and the poles of P_0 in equation (16) merge, i.e.

$$c_i \overset{E\to\infty}{\longrightarrow} a_i. \tag{18}$$

We simplify the formal WKB solution of equation (15)

$$f_1^{(n)} = \frac{1}{\sqrt[4]{P_0}}\exp\left(\mp \mathrm{i}\int^p \sqrt{P_0}\,\mathrm{d}p\right) \qquad n=1,2 \tag{19}$$

in the high-energy limit ($(U_1-U_2)^2E^{-1} \ll 1$):

$$\sqrt{P_0} \simeq \frac{\nu}{p} + \delta_1\frac{2p}{p^2-a_1} + \delta_2\frac{2p}{p^2-a_2} + \mathrm{O}(\delta^2) \qquad \sqrt[4]{P_0} \simeq \sqrt{\frac{\mu}{p}}. \tag{20}$$

The energy-dependent parameters δ's in equation (20) are defined in terms of the mixing angle in the limit of asymptotically forbidden region,

$$\begin{aligned} &\delta_i \simeq \mu\frac{a_i-c_i}{4a_i} = \tfrac{1}{2}\delta\,(1\pm\cos(2\theta(-\infty))) \\ &\delta = \delta_1+\delta_2 \simeq \tfrac{1}{2}(\mu-\nu). \end{aligned} \tag{21}$$

In order to be consistent with the WKB wavefunction in equation (19), we also replace the Hankel function in equation (10) with its WKB approximation (cf equation (A5) of the appendix). Then the contour integral of equation (10) contains the phase integral given by

$$S(\rho,\ p) = \int^p \sqrt{P_0(p)}\,\mathrm{d}p - \int^{\rho p}\sqrt{1+\frac{\nu^2}{\xi^2}}\,\mathrm{d}\xi. \tag{22}$$

The main contribution comes from the saddle points $p_j^\dagger(\rho)$ defined by

$$\frac{\partial}{\partial p}S(\rho,\ p)\bigg|_{p=p_j^\dagger} = 0 \tag{23}$$

and given explicitly by

$$\left(p_j^\dagger(\rho)\right)^2 = \frac{\beta_1+\beta_2}{2} - \frac{\nu^2-\mu^2}{2\rho^2} \pm \sqrt{\left(\frac{\beta_1-\beta_2}{2}-\frac{\mu^2-\nu^2}{2\rho^2}\right)^2+1} \qquad j=1,2. \tag{24}$$

Because of this ρ–p correspondence the above action simply becomes

$$S\left(\rho,\ p_j^\dagger(\rho)\right) = \int^x \sqrt{E-u_j^{(a)}(x)}\,\mathrm{d}x \equiv S_j(\rho). \tag{25}$$

The procedure in this section defines the approximation which is used to solve the present exponential model. We cut the complex p-plane along the four branch cuts of $(P_0)^{1/2}$ chosen on the imaginary axis

$$\left(\mathrm{i}\sqrt{|c_j|},\ \mathrm{i}\sqrt{|a_j|}\right) \qquad \left(-\mathrm{i}\sqrt{|a_j|},\ -\mathrm{i}\sqrt{|c_j|}\right) \qquad j=1,2. \tag{26}$$

3. Semiclassical wavefunctions

Since we deal with two coupled differential equations of the second order, we first represent the total wavefunction as a linear combination of four fundamental solutions given by some, as yet unknown, contour integrals. Then we evaluate these integrals in the limits $x \to \mp\infty$ and determine the four constants of this linear combination. When x lies in the classically inaccessible region, we obtain two restrictions on these constants because of the decay of the wavefunction in each adiabatic channel. Evaluating the contour integrals for $x \to \infty$, we obtain the asymptotic form of the wavefunction. In order to obtain the **S**-matrix we set one more condition that the total wavefunction is of a form such that the incident wave propagates only in one channel. Then the last constant is just a multiplicative factor of the total wavefunction. Thus we can finally obtain the **S**-matrix.

3.1. Independent solutions

At $x \to \infty$, the independent solutions in the adiabatic representation should behave like

$$\phi_1(\rho) \sim \rho^{\pm i\nu} \sim e^{\mp ik_1 x} \qquad \text{and} \qquad \phi_2(\rho) \sim \rho^{\pm i\mu} \sim e^{\mp ik_2 x} \qquad (\rho \to 0). \tag{27}$$

In the classically inaccessible region they correspond to exponentially growing functions, in general,

$$\phi_1(\rho) \sim \exp\left(|\sqrt{a_1}|\rho\right) \qquad \phi_2(\rho) \sim \exp\left(|\sqrt{a_2}|\rho\right) \qquad (\rho \to \infty). \tag{28}$$

Equation (27) follows from the fact that the diabatic potentials are asymptotically flat and the coupling vanishes, while equation (28) can be obtained by solving the Schrödinger equation with the diagonal adiabatic potential matrix (we note that the rotation angle in equation (6) tends to a constant). If only the leading-order term is retained, then we have

$$\left[\rho^2 \frac{d^2}{d\rho^2} + a_i\right] \phi_i(\rho) \simeq 0. \tag{29}$$

In equation (28) the exponentially decreasing terms have been omitted, since they are only subdominant in the region. Taking into account equations (27) and (28), we can represent the wavefunction in equation (10) as

$$\psi_j(\rho) = \sum_{m,n=1}^{2} \gamma_{mn} I_{mn}^{(j)}(\rho) \tag{30}$$

where

$$I_{mn}^{(j)}(\rho) \equiv \int_{C_{mn}} dp\, p F_j^{(n)}(p)\, Z^{(n)}(\rho p). \tag{31}$$

Here $F_j^{(n)}$ are derived from equation (19), using equations (12) and (13). The first index m indicates which couple of symmetric branch cuts is wound around by the contour, while the index n specifies in which complex half-plane the branch is located:

$$\begin{aligned} &n = 1 \qquad Z^{(n)} = H_{-i\nu}^{(1)} \qquad \text{lower branch cut} \\ &n = 2 \qquad Z^{(n)} = H_{i\nu}^{(2)} \qquad \text{upper branch cut.} \end{aligned} \tag{32}$$

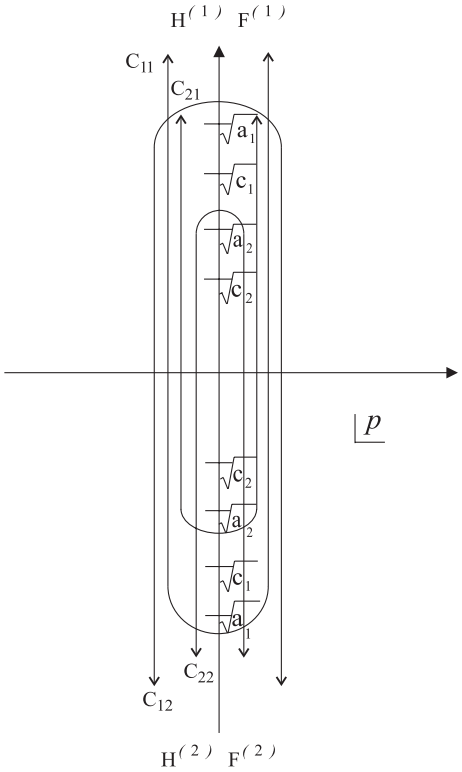

Figure 1. Bessel transformation contours in the complex p-plane. Two contours (C_{i1}, $i = 1, 2$) wind the branch cuts at the lower complex half-plane of p and go to $+\mathrm{i}\infty$, while the two others (C_{i2}, $i = 1, 2$) wind the branch cuts at the upper half-plane and go to $-\mathrm{i}\infty$. The numbering of contours, C_{ij}, corresponds to the Hankel functions, $H^{(j)}$, and the WKB wavefunctions, $F^{(j)}$.

The case $n = 1$ ($n = 2$) corresponds to the contour tips at $p = +\mathrm{i}\infty$ ($p = -\mathrm{i}\infty$) as shown in figure 1. From this figure and equations (10), (19) and (A5) it follows that

$$I^{(j)}_{mn} = \left(I^{(j)}_{m,3-n}\right)^{\star}. \tag{33}$$

This condition ensures the unitarity of the **S**-matrix. The saddle-point analysis, carried out in the high-energy limit [14], proves that the main contribution to the integrals in equation (30) comes from regions in the complex p-plane such that

$$z = \rho p \sim 0 \qquad \text{for} \quad \rho \to 0 \tag{34}$$

and

$$|z| = |\rho p| \sim \infty \qquad \text{for} \quad \rho \to \infty.$$

This allows us to expand the Bessel function $H_{\pm\mathrm{i}\nu}(z)$ in equation (10) (cf equations (A1) and (A2) in the appendix). Equation (27) follows from the transformation based on $H_{\pm\mathrm{i}\nu}(z)$ (or alternatively on $H_{\pm\mathrm{i}\mu}(z)$). In the limit $\rho \to \infty$ the saddle points tend to $\sqrt{a_i}$ (cf equations (14) and (24)), which gives equation (28). Thus the conditions in equations (27) and (28) can be satisfied by our choice of contours and wavefunctions.

3.2. Wavefunction at $x \to -\infty$

In order to derive the wavefunction in the forbidden region, we perform the standard procedures, i.e. analysis of the singularities, solution of the comparison equation and asymptotic matching

[1, 7, 16]. The total wavefunction

$$\Phi(\rho) = \begin{pmatrix} \phi_1 \\ \phi_2 \end{pmatrix} \tag{35}$$

should not contain exponentially growing terms at $\rho \to \infty$. In order to satisfy this physical condition we first evaluate the integrals $I^{(j)}_{nm}(\rho)$ of equation (30) for $\rho \to \infty$. To do this, we first have to match the local solution of equation (15) at $p \sim \sqrt{a_i}$ to the WKB solution equation (19). The procedure is explained in appendices B and C, and the final expressions of $I^{(j)}_{nm}(\rho)$ are given in equations (D3) and (D4). Then we rotate the diabatic wavefunctions $\psi_j(x)$ given by equation (30) into the adiabatic ones $\phi_j(x)$ using the matrix in equation (6) (cf equation (D5) in the appendix). To cancel the contribution of exponentially diverging terms in adiabatic wavefunctions in equation (28), the following condition should be satisfied (cf equation (D7) in the appendix):

$$\frac{\gamma_{12}}{\gamma_{11}} = \exp(\mathrm{i}\alpha_1) \qquad \frac{\gamma_{22}}{\gamma_{21}} = \exp(\mathrm{i}\alpha_2) \tag{36}$$

where

$$\alpha_i = -2\left(\arg(\Gamma(\mathrm{i}\delta_i)) + \delta_{3-i}\ln(a_2 - a_1) + \tfrac{1}{2}\nu\ln(-a_i) + \delta_i \ln\left(\frac{-a_i}{\mu}\right)\right). \tag{37}$$

3.3. Wavefunction at $x \to \infty$

Evaluating integrals in equation (31) at $\rho \to 0$, we find the total wavefunction

$$\begin{aligned}\psi_1(\rho) = {} & \pi\frac{\rho^{\mathrm{i}\nu}}{\sqrt{\nu}}\mathrm{e}^{\mathrm{i}(\phi_0+\pi/4)}\frac{\Gamma(1+\mathrm{i}\delta)(a_2-a_1)^{-\mathrm{i}\delta-1}}{\Gamma(1+\mathrm{i}\delta_1)\Gamma(1+\mathrm{i}\delta_2)}\left(-\mathrm{e}^{\pi\delta_2}\gamma_{11} + \mathrm{e}^{-\pi\delta_2}\gamma_{21}\right) \\ & +\pi\frac{\rho^{-\mathrm{i}\nu}}{\sqrt{\nu}}\mathrm{e}^{-\mathrm{i}(\phi_0+\pi/4)}\frac{\Gamma(1-\mathrm{i}\delta)(a_2-a_1)^{\mathrm{i}\delta-1}}{\Gamma(1-\mathrm{i}\delta_1)\Gamma(1-\mathrm{i}\delta_2)}\left(-\mathrm{e}^{\pi\delta_2}\gamma_{12} + \mathrm{e}^{-\pi\delta_2}\gamma_{22}\right)\end{aligned} \tag{38}$$

and

$$\begin{aligned}\psi_2(\rho) = {} & -\mathrm{i}\frac{\rho^{\mathrm{i}\mu}}{\sqrt{\mu}}\mathrm{e}^{\mathrm{i}(\phi_0-\delta\ln(4\nu)-\pi/4)}\Gamma(-\mathrm{i}\delta)\mathrm{e}^{\pi\delta/2}\left(\mathrm{e}^{-\pi\delta_1}\,\mathrm{sh}(\pi\delta_1)\gamma_{11} + \mathrm{e}^{-\pi\delta_2}\,\mathrm{sh}(\pi\delta_2)\gamma_{21}\right) \\ & +\mathrm{i}\frac{\rho^{-\mathrm{i}\mu}}{\sqrt{\mu}}\mathrm{e}^{-\mathrm{i}(\phi_0-\delta\ln(4\nu)-\pi/4)}\Gamma(\mathrm{i}\delta)\mathrm{e}^{\pi\delta/2}\left(\mathrm{e}^{-\pi\delta_1}\,\mathrm{sh}(\pi\delta_1)\gamma_{12} + \mathrm{e}^{-\pi\delta_2}\,\mathrm{sh}(\pi\delta_2)\gamma_{22}\right)\end{aligned} \tag{39}$$

where Γ is the gamma function [15] and the phase factor

$$\phi_0 \equiv \nu\ln\left(\frac{e}{2\nu}\right) \tag{40}$$

comes from the expansion of Hankel and gamma functions (cf equations (A2) and (A4) in the appendix).

The details of how to evaluate $\psi_j(\infty)$ are given in appendix E (cf equations (E4) and (E6)).

4. Scattering matrix and non-adiabatic transition matrix

In this section we first derive the scattering matrix containing parameters of the present exponential potential model. Then we evaluate the adiabatic scattering phase shifts in order to subtract the non-adiabatic transition probability and dynamical phases, using the idea of double passage. Finally, the total S-matrix can be put in a form which is free from the particular parameters of our model.

4.1. Scattering matrix

Let us first denote the adiabatic momenta,

$$k_i(x) = \sqrt{E - u_i^{(a)}(x)} \qquad \text{and} \qquad k_i \equiv \lim_{x\to\infty} k_i(x). \tag{41}$$

Then the scattering matrix in the present case is defined as

$$\begin{array}{l|l} \text{channel } \psi_i & \text{channel } \psi_j \\ \leftarrow 1 & \leftarrow 0 \\ \rightarrow -S_{ii} & \rightarrow -S_{ij} \end{array} \tag{42}$$

where the arrows mean

$$\left.\begin{array}{l} \overleftarrow{\text{incoming wave}} \\ \overrightarrow{\text{outgoing wave}} \end{array}\right\} \frac{\exp(\mp \mathrm{i} k_j x)}{\sqrt{k_j}} \qquad \text{or} \qquad \frac{\exp(\mp \mathrm{i}\int_{x_j^t}^{x} k_j(x)\,\mathrm{d}x)}{\sqrt{k_j}} \tag{43}$$

and x_j^t represents the turning point. While the plane waves in equation (43) are connected by the scattering matrix, $\mathbf{S}(E)$, the latter adiabatic waves define the reduced scattering matrix, $\mathbf{S}^R(E)$.

The matrix $\mathbf{S}(E)$ can be deduced from $\Psi(x)|_{x\to\infty}$ as explained below. In equations (38) and (39) the four parameters γ_{ij} are restricted by the two conditions from equations (36). We impose one more restriction on γ_{ij} in order to specify the only outgoing wave boundary condition in the first channel (to obtain S_{2j} elements) or in the second channel (to obtain S_{1j} elements). Thus all γ_{ij} can be found up to a multiplicative constant and the **S**-matrix elements are evaluated using equations (36), (38) and (39) as follows:

$$\begin{aligned} S_{11}(E) = {} & \mathrm{i}\exp\big(2\mathrm{i}\big[\delta \ln(a_2 - a_1) + \arg(\Gamma(\mathrm{i}\delta_1)) + \arg(\Gamma(\mathrm{i}\delta_2)) - \arg(\Gamma(\mathrm{i}\delta))\big]\big) \\ & \times \exp\big(2\mathrm{i}\big[-\phi_0 - \nu \ln(2\sqrt{V})\big]\big)\left(p\mathrm{e}^{\mathrm{i}\alpha_2} + (1-p)\mathrm{e}^{\mathrm{i}\alpha_1}\right) \end{aligned} \tag{44a}$$

$$\begin{aligned} S_{12}(E) = {} & -\mathrm{i}\frac{\sqrt{\delta_1\delta_2}}{\pi}\frac{\sinh(\pi\delta_1)\sinh(\pi\delta_2)\,\Gamma(\mathrm{i}\delta_1)\,\Gamma(\mathrm{i}\delta_2)}{\sinh(\pi\delta)}\mathrm{e}^{\pi(\delta_1-\delta_2)/2} \\ & \times \exp\big(\mathrm{i}\big[\delta \ln(4\nu(a_2 - a_1)) - 2\phi_0 - (\nu+\mu)\ln(2\sqrt{V})\big]\big)\left(\mathrm{e}^{\mathrm{i}\alpha_2} - \mathrm{e}^{\mathrm{i}\alpha_1}\right) \end{aligned} \tag{44b}$$

$$\begin{aligned} S_{21}(E) = {} & -\mathrm{i}\frac{\pi}{\sqrt{\delta_1\delta_2}}\frac{\exp\big(\mathrm{i}\big[\delta \ln\big(4\nu(a_2 - a_1)\big) - 2\phi_0 - (\nu+\mu)\ln(2\sqrt{V})\big]\big)}{\sinh(\pi\delta)\Gamma\big(-\mathrm{i}\delta_1\big)\Gamma\big(-\mathrm{i}\delta_2\big)}\mathrm{e}^{\pi(\delta_1-\delta_2)/2} \\ & \times\left(\mathrm{e}^{\mathrm{i}\alpha_2} - \mathrm{e}^{\mathrm{i}\alpha_1}\right) \end{aligned} \tag{44c}$$

and

$$S_{22}(E) = \mathrm{i}\exp\big(2\mathrm{i}\big[-\phi_0 + \delta \ln(4\nu) + \arg(\Gamma(\mathrm{i}\delta)) - \mu\ln(2\sqrt{V})\big]\big)\left(p\mathrm{e}^{\mathrm{i}\alpha_1} + (1-p)\mathrm{e}^{\mathrm{i}\alpha_2}\right) \tag{44d}$$

where

$$p = \exp(-\pi\delta_2)\frac{\sinh(\pi\delta_1)}{\sinh(\pi\delta)}. \tag{45}$$

The **S**-matrix given above satisfies symmetry and unitarity (cf equations (F1)–(F7) in the appendix). The total transition probability $|S_{12}|^2$ is given by

$$|S_{12}(E)|^2 = 4\frac{\exp(\pi\delta)\sinh(\pi\delta_1)\sinh(\pi\delta_2)}{\big[\exp(\pi\delta)\sinh(\pi\delta_2) + \sinh(\pi\delta_1)\big]^2}\sin^2\left(\tfrac{1}{2}(\alpha_2 - \alpha_1)\right). \tag{46}$$

4.2. Double passage

With use of the idea of the double passage, the **S**-matrix can be expressed as a product of the non-adiabatic transition matrix and the adiabatic propagation matrix [3, 7, 9, 10]. The non-adiabatic transition matrix connects the WKB wavefunctions

$$\frac{1}{\sqrt{k_i(x)}}\exp\left(\mathrm{i}\int_{x_s}^{x} k_i(y)\,\mathrm{d}y\right) \tag{47}$$

from left to the right, both far from the reference point x_s. It generally has the form

$$\mathbf{I}(x_s) = \begin{pmatrix} \sqrt{1-p}\exp(-\mathrm{i}\phi) & -\sqrt{p}\exp(-\mathrm{i}\psi) \\ \sqrt{p}\exp(\mathrm{i}\psi) & \sqrt{1-p}\exp(\mathrm{i}\phi) \end{pmatrix} \tag{48}$$

where p is the non-adiabatic transition probability for one passage of the transition region, and ψ and ϕ are the dynamical phases. If the turning points are well separated from the transition region and the WKB approximation does not break, then the **S**-matrix is decomposed to have the following double-passage form:

$$\begin{aligned} S_{11} &= \mathrm{i}\exp(\mathrm{i}(2(d_1-\phi)-\Phi_{12}))\left((1-p)\,\mathrm{e}^{\mathrm{i}\Phi_{12}} + p\,\mathrm{e}^{-\mathrm{i}\Phi_{12}}\right) \\ S_{22} &= \mathrm{i}\exp(\mathrm{i}(2(d_2+\phi)+\Phi_{12}))\left((1-p)\mathrm{e}^{-\mathrm{i}\Phi_{12}} + p\,\mathrm{e}^{\mathrm{i}\Phi_{12}}\right) \end{aligned} \tag{49}$$

and

$$S_{12} = S_{21} = -2\exp(\mathrm{i}(d_1+d_2))\sqrt{p(1-p)}\sin(\Phi_{12})$$

where

$$\Phi_{12} = \Delta_1 - \Delta_2 + \psi - \phi. \tag{50}$$

The quantities d_i are the adiabatic elastic scattering phase shifts and Δ_i are the adiabatic scattering phases from the turning points to the reference point $x_s = \mathrm{Re}\,x_*$, where x_* is the complex crossing point (see equation (54) below). Our goal now is to subtract the parameters p, ϕ and ψ from equations (44*a*)–(44*d*) using this double-passage formula. It is easy to see that p of equation (45) is the non-adiabatic transition probability in equation (49), which has the same form as in the attractive case. Indeed, in the case of asymptotically high energies the transition probability should not depend on the sign of potential slopes. Comparing equations (44*a*)–(44*d*) and (49) we can also identify Φ_{12} of equation (50) as

$$2\Phi_{12} = \alpha_2 - \alpha_1. \tag{51}$$

To obtain explicit expressions of ϕ and ψ it is necessary to evaluate the phase shift integrals on the adiabatic potentials, d_i and Δ_i. The exact results cannot be obtained analytically but we can obtain analytical results within the high-energy expansion. For this purpose we make use of equation (22).

The adiabatic elastic scattering phase shifts are defined by

$$d_i \equiv \left(\lim_{X\to\infty}\int_{x_i^t}^{X}\sqrt{E-u_i^{(a)}(x)}\,\mathrm{d}x - X\sqrt{E-U_i}\right). \tag{52}$$

The phase shifts between the reference point and the turning points are given as

$$\Delta_i \equiv \int_{x_i^t}^{x_s}\sqrt{E-u_i^{(a)}(x)}\,\mathrm{d}x. \tag{53}$$

In order to represent the scattering matrix in the double-passage form we choose the reference point as a real part of the complex crossing point of adiabatic potentials,

$$x_s \equiv \operatorname{Re} x_* = -\ln\left(\frac{(U_1 - U_2)/(2|V|)}{\sqrt{1 + \left(\frac{1}{2}(\beta_1 - \beta_2)\right)^2}}\right). \tag{54}$$

In addition to this we modify equation (22) to the following form:

$$\int_{x_j^t}^{x} \sqrt{E - u_j^{(a)}(y)}\,\mathrm{d}y = \int_{\sqrt{c_j}}^{p_j^{\dagger}(\rho)} \sqrt{P_0(p)}\,\mathrm{d}p - \int_{\mathrm{i}\nu}^{\rho p_j^{\dagger}(\rho)} \sqrt{1 + \frac{\nu^2}{\xi^2}}\,\mathrm{d}\xi \tag{55}$$

and note that

$$p_1^{\dagger}(\rho) \xrightarrow{\rho\to 0} \sqrt{\beta_1}$$

$$p_2^{\dagger}(\rho) \xrightarrow{\rho\to 0} \sqrt{\mu^2 - \nu^2}/\rho.$$

Equations (54) and (55) enable us to evaluate the phases in equations (52) and (53). The results follow (cf equations (G1)–(G7) in the appendix)

$$d_1 = \nu\ln\nu - \nu - \tfrac{1}{2}\nu\ln|V| - \tfrac{1}{2}\nu\ln|a_1| - \delta_1\ln\left|\frac{a_1}{\mu}\right| + \delta_1 - \delta_1\ln\sqrt{\delta_1\delta_2} + \delta_2\ln\frac{\delta_2}{\delta} \tag{56}$$

$$d_2 = \mu\ln\mu - \mu - \tfrac{1}{2}\mu\ln|V| - \tfrac{1}{2}\mu\ln|a_2| + \delta_1\ln\left|\frac{a_2}{\mu}\right| - \delta_1 + \delta_1\ln\sqrt{\delta_1\delta_2} - \delta_2\ln\frac{\delta_2}{\delta} \tag{57}$$

and

$$\Delta_1 - \Delta_2 = \frac{\nu}{2}\ln\left(\frac{a_2}{a_1}\right) + \delta\ln\frac{a_2}{a_1} + \delta_1 - \delta_1\ln\frac{\delta_1}{\mu} + \delta_2\ln|a_1| + (\delta_1 - \delta_2)\ln\frac{\delta}{\sqrt{\delta_1\delta_2}}$$
$$-\delta_2 + \delta_2\ln\frac{\delta_2}{\mu} - \delta_1\ln|a_2| - \operatorname{Re}\left\{\int_{\operatorname{Re}x_*}^{x_*}(k_1(x) - k_2(x))\,\mathrm{d}x\right\}. \tag{58}$$

4.3. The general **S***-matrix*

Identifying p of the **S**-matrix formula with that of the **I**-matrix we can find the dynamical phases. First we substitute equations (56)–(58) into the double-passage formula in equation (49). The dynamical phases follow when comparing the result with the **S**-matrix in equations (44*a*)–(44*d*). We use the notation

$$\gamma(X) = X\ln(X) - X - \arg(\Gamma(\mathrm{i}X)) \tag{59}$$

in terms of which the dynamical phases result in

$$\phi = \gamma(\delta_2) - \gamma(\delta) \tag{60}$$

and

$$\psi = \gamma(\delta_1) - \gamma(\delta) - 2\left[\sqrt{\delta\delta_2} + \frac{\delta_1}{2}\ln\frac{\sqrt{\delta} - \sqrt{\delta_2}}{\sqrt{\delta} + \sqrt{\delta_2}}\right]. \tag{61}$$

The phases ψ and ϕ, unlike from the previous **S**-matrix in equations (44*a*)–(44*d*), depend only on the positive parameters δ_i. The same holds for the non-adiabatic transition probability p in equation (45). Let us mention here the explicit dependence of δ_i on the parameters of

the exponential model before introducing the dimensionless variables (cf the sentence below equation (2)). As follows from equations (8) and (21),

$$\delta \simeq \frac{\sqrt{2M}}{\hbar\alpha}\left(\sqrt{E-U_2}-\sqrt{E-U_1}\right). \tag{62}$$

Furthermore, we show that δ_i can be considered as being free from the particular parameters of the exponential model.

We have proven above that the total **S**-matrix can be put into a general form

$$S_{ij}(E) = \lim_{x\to\infty} \exp\left(-\mathrm{i}(k_i(\infty)+k_j(\infty))x\right)\left[\mathbf{P}(x,x_s)\mathbf{I}(x_s;\ E)\mathbf{P}(x_s,x^t)\right.$$
$$\left.\mathrm{i}\mathbf{P}^*(x^t,x_s)\mathbf{I}^t(x_s;\ E)\mathbf{P}^*(x_s,x)\right]_{ij} \tag{63}$$

where the diagonal matrix P represents the uncoupled adiabatic propagation,

$$P_{ij}(b,a) = \delta_{ij}\exp\left(\mathrm{i}\int_{a_j}^{b_j} k_j(y)\,\mathrm{d}y\right). \tag{64}$$

Finally, the non-adiabatic transition matrix **I** is given by equation (48), with the parameters p, ϕ and ψ defined in equations (45), (60) and (61). $\mathbf{I}^t$ in equation (63) is a transpose of **I** and $\mathbf{P}^*$ is a complex conjugate of the matrix in equation (64). The energy-dependent parameters $\delta_i(E)$ are nothing but contour integrals of adiabatic momenta in the complex coordinate plane. In the attractive case they have the following form [14]:

$$\delta_1 = \frac{1}{\pi}\,\mathrm{Im}\left\{\int_{x_1^t}^{x_*} k_1(x)\,\mathrm{d}x - \int_{x_2^t}^{x_*} k_2(x)\,\mathrm{d}x\right\} \tag{65}$$

and

$$\delta_2 = \frac{1}{\pi}\,\mathrm{Im}\left\{\int_{\mathrm{Re}(x_*)}^{x_*} [k_2(x)-k_1(x)]\,\mathrm{d}x\right\} \tag{66}$$

where x_i^t are the turning points (complex in the attractive case) and x_* is the crossing point of adiabatic potentials in the complex plane. For the proof of equations (65) and (66) refer to equations (H1)–(H5) in the appendix and figures 2–4.

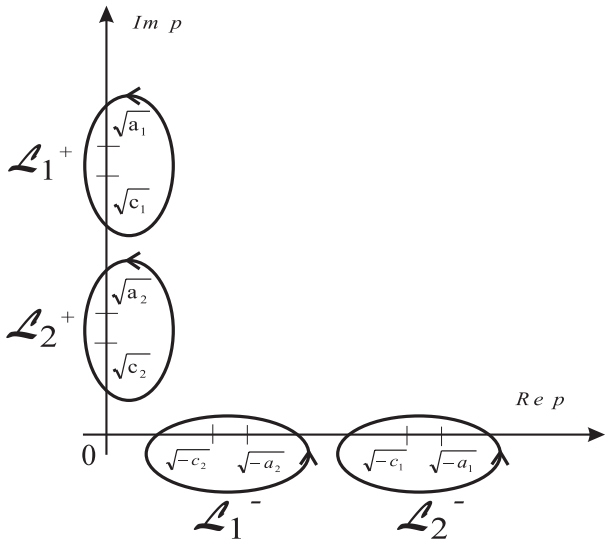

Figure 2. Contours L_i. The two contours L_1 and L_2 define the parameters δ_i of equations (65) and (66) in the complex p-plane. These are shown both for the repulsive case, L_i^+ (branch cuts on the imaginary axis) and for the attractive case, L_i^- (branch cuts on the real axis), (see equation (H6)).

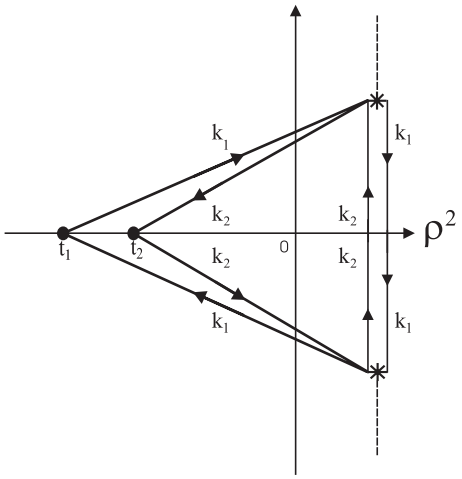

Figure 3. Contours in the complex ρ^2-plane (attractive case). The two closed contours correspond to L_1^- and L_2^- of figure 2 when transformed to the ρ^2-plane. The bold line is the contour for δ_1, while the contour for δ_2 (thin line) winds around the complex crossing points denoted by stars. The adiabatic momenta, integrated on the respective parts of the contours, are denoted as k_1 and k_2, and t_i $(i = 1, 2)$ denotes the corresponding turning points $-v^2/c_i$. Branch cuts of adiabatic potentials are plotted as a broken line. The overall integration result, $\delta = \delta_1 + \delta_2$, is the sum of integrals of k_1 and k_2 on two contours that encircle $\rho^2 = 0$ $(x = \infty)$ in opposite directions.

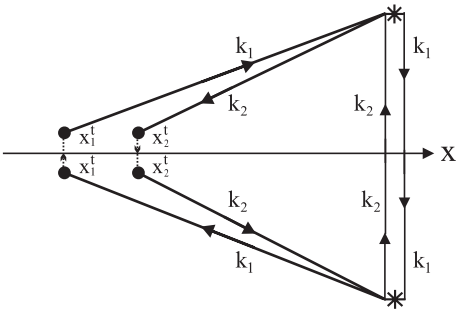

Figure 4. Contours in the complex coordinate plane (attractive case). The contours for δ_i in the x-plane. Turning points x_i^t are located out of the real axis. As a result the integral for δ can be reduced to the integration on the dotted contours. In the repulsive case $\mathrm{Im}\, x_i^t = 0$, the complex conjugate turning points merge together, and the sum of the two contour integrals equals zero.

In the repulsive case we have found (cf equations (H6)–(H13) in the appendix) that

$$\delta_1 = \frac{1}{\pi}\,\mathrm{Im}\left\{\int_{\mathrm{Re}(x_*)}^{x_*} [k_2(x) - k_1(x)]\,\mathrm{d}x\right\} \equiv \delta_{LZ} \tag{67}$$

and

$$\delta_2 = \delta - \delta_{LZ} \tag{68}$$

where

$$\delta = \tfrac{1}{2}(\mu - \nu) \equiv \delta_{RZ}. \tag{69}$$

The Rozen–Zener parameter in the above equation can be expressed as follows:

$$\delta_{RZ} = \frac{1}{2\pi\mathrm{i}} \oint_{\infty} [k_2(x) - k_1(x)]\,\mathrm{d}x \tag{70}$$

as can be seen when introducing a new variable, $z = \mathrm{e}^{-x}$. Finally, based on the symmetries between the attractive and repulsive case (cf equation (H7) in the appendix), the formulae in equations (67) and (68) are equivalent to

$$\delta_1 = \frac{1}{\pi}\,\mathrm{Im}\left\{\int_{\mathrm{Re}(x_*)}^{x_*} [k_2(x + \mathrm{i}\pi) - k_1(x + \mathrm{i}\pi)]\,\mathrm{d}x\right\} \tag{71}$$

and

$$\delta_2 = \frac{1}{\pi}\,\mathrm{Im}\left\{\int_{x_1^t}^{x_*} k_1(x+\mathrm{i}\pi)\,\mathrm{d}x - \int_{x_2^t}^{x_*} k_2(x+\mathrm{i}\pi)\,\mathrm{d}x\right\}. \tag{72}$$

These formulae have a very illustrative meaning. In figure 4 (attractive case) we can see that the parameter $\delta = \delta_1 + \delta_2$ is given by the two contour integrals of adiabatic momenta between the adjacent complex turning points. In the repulsive case, however, the pairs of turning points degenerate on the real axis (regardless of the exponential model) and the only independent contour integral is that for δ_{LZ}. We found that this problem can be generally solved by inverting the potential,

$$u_i^{(a)}(x)|_{attr} = u_i^{(a)}(\infty) - \left(u_i^{(a)}(x) - u_i^{(a)}(\infty)\right) \tag{73}$$

and substituting the corresponding adiabatic momenta $k_i(x)|_{attr}$ into equations (71) and (72) instead of $k_i(x+\mathrm{i}\pi)$. It is well known in semiclassical analysis that the results for the attractive and repulsive cases do not differ in the high-energy limit if we take

$$u_i^{(a)}(x)|_{attr} = -u_i^{(a)}(x)|_{rep}. \tag{74}$$

The advantage of the above formulae, however, is (a) that their validity does not require an energy much greater than the asymptotic separation of adiabatic potential energy levels and (b) that they can be used in a model-independent way. Such an achievement is quite substantial as we demonstrate in the next section. This is due to the contour integral definition of the substantial parameters δ_1 and δ_2 which enables us to apply the above formulae for energies even quite significantly below the diabatic crossing point.

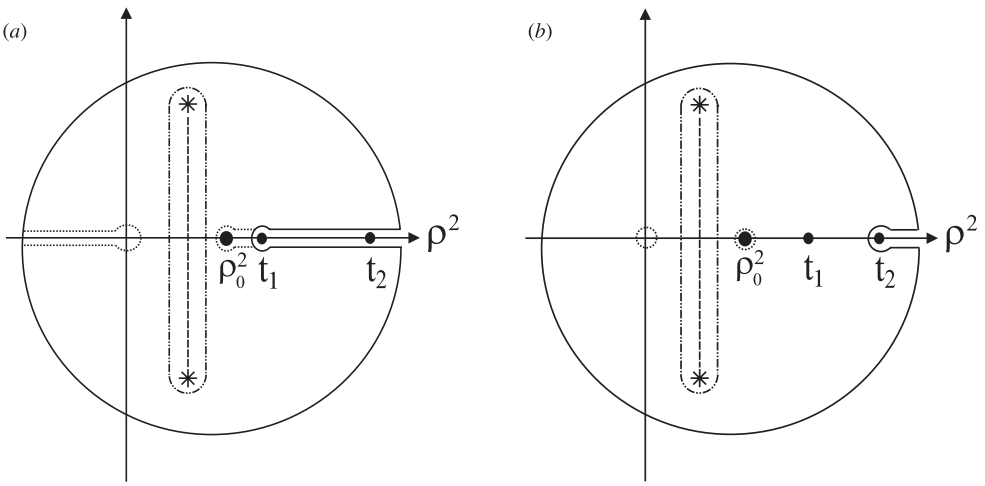

Figure 5. Contours in the complex ρ^2-plane (repulsive case). (*a*) Integral for δ_1. The full curve corresponds to the contour L_1^+ (cf equation (H2) with $i = 1$). The dotted curve shows how the contour can be distorted without changing the integration result (see equation (H10)). The point ρ_0^2 corresponds to $p_2^\dagger = 0$ which does not contribute to δ_1 (see equation (H4)). Stars denote the adiabatic crossing points which are connected by a branch cut (broken curve), t_1 and t_2 are the turning points. The contour for δ_1 can be finally reduced to the double-dot-broken curve. (*b*) Integral for δ_2. Not only the same contour (double-dot-broken) as in (*a*) except that $i = 2$ in equation (H2) but also the closed dotted contours arising from equations (H11) and (H4) contribute to δ_2.

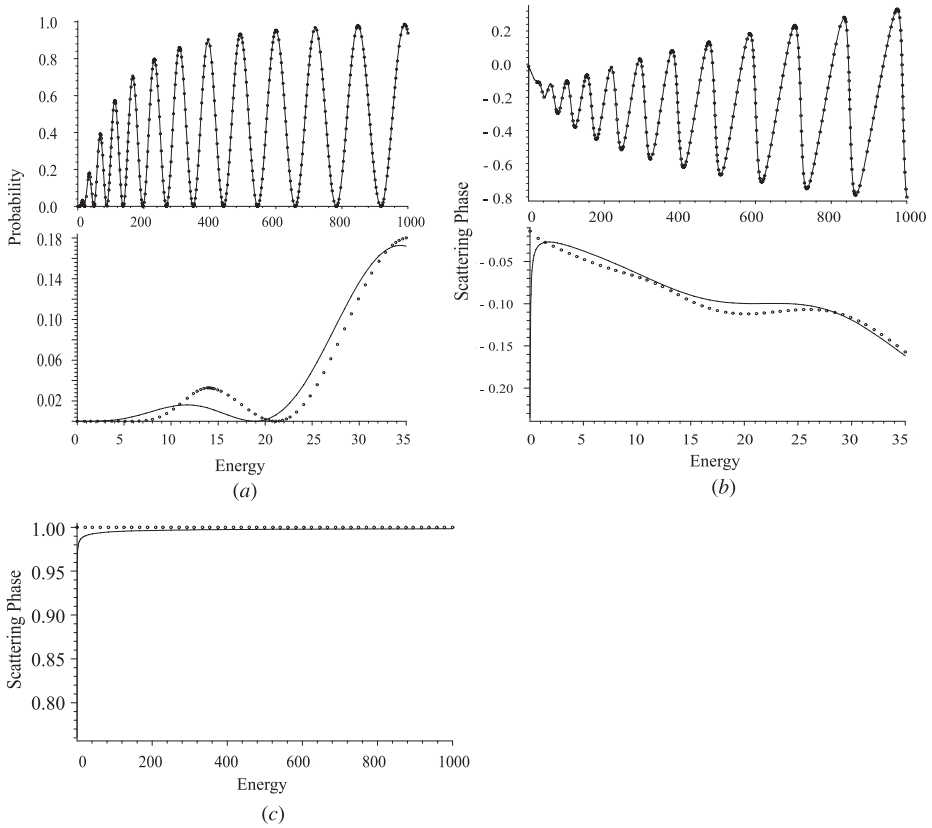

Figure 6. Accuracy of the semiclassical S^R matrix. (*a*) The transition probability $P(E)$ (see equation (76)). (*b*) The scattering phase $\Phi(E)$ (see equation (77)). (*c*) The scattering phase $\Psi(E)$ (see equation (78)). In (*a*)–(*c*) the lower plot is a detail of the upper one. The potential parameters are $V_1 = -30$, $V_2 = -40$, $V = 20$, $U_1 = 0$ and $U_2 = -15$, which represent a system with large asymptotic energy level separation. That is why the condition in equation (75) is fulfilled for the energy which is above the scale in this figure. The total transition probability (equation (76)) and the rescaled S^R-matrix phases (equations (77) and (78)) are plotted against the dimensionless energy. The full curve is the exact quantum solution and the circles show the analytical result from equation (63). The energy of the diabatic crossing point is 45, while the energy at the reference point (the average of adiabatic potentials) is ~ 5.2.

5. Numerical examinations

We expect that the high energy is the critical factor for the accuracy of the present semiclassical treatment (see equation (20)). It means

$$E > \frac{(\Delta U)^2}{\delta^2} \qquad \delta \to 0 \tag{75}$$

when we neglect quantities $\sim \delta^2$. However, we found that the results in equations (44*a*)–(44*d*) are far more accurate than it could follow from equation (75). It is amazing that the theory works even when the energy is below the crossing point of the diabatic potentials. Using the general formulae in equations (65) and (66) we could extend the validity region of our results

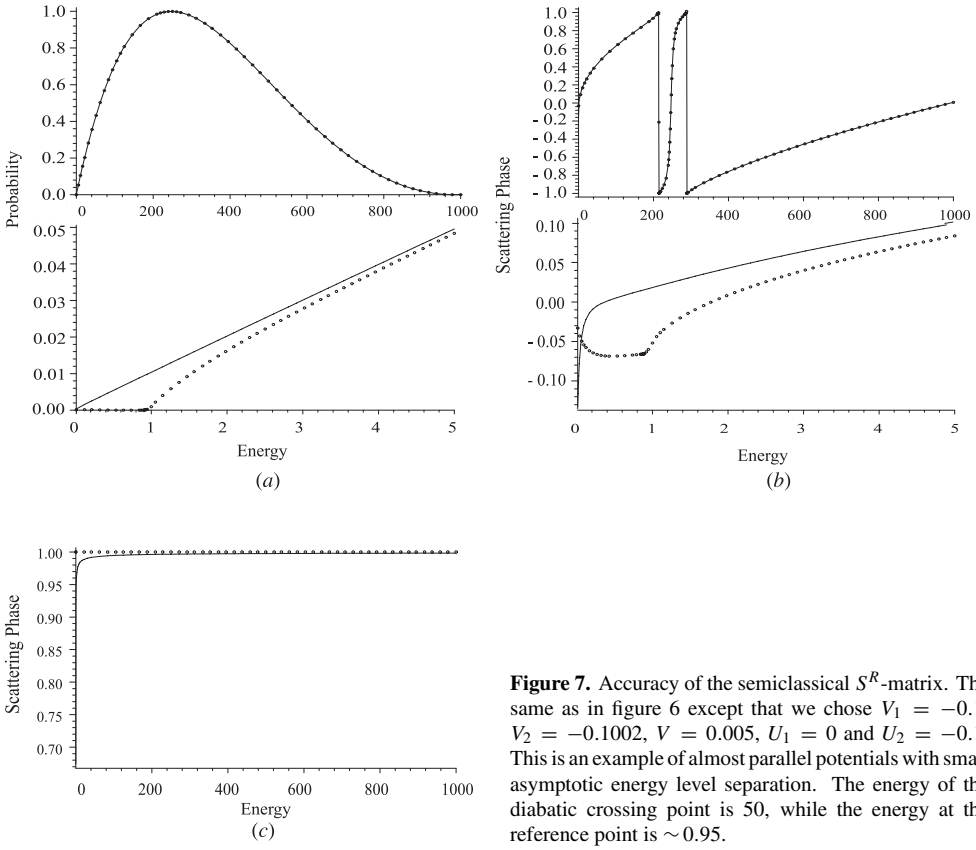

Figure 7. Accuracy of the semiclassical S^R-matrix. The same as in figure 6 except that we chose $V_1 = -0.1$, $V_2 = -0.1002$, $V = 0.005$, $U_1 = 0$ and $U_2 = -0.1$. This is an example of almost parallel potentials with small asymptotic energy level separation. The energy of the diabatic crossing point is 50, while the energy at the reference point is ~ 0.95.

to a larger range of energy. Particular examples are given in figures 6 and 7. The following three quantities are shown in these figures:

$$P(E) = \left|S_{12}^R(E)\right|^2 \tag{76}$$

$$\Phi(E) = \frac{1}{\pi} \arg\left\{\frac{S_{11}^R(E)}{S_{22}^R(E)}\right\} \tag{77}$$

and

$$\Psi(E) = \frac{1}{\pi} \arg\left\{S_{11}^R(E) S_{22}^R(E)\right\}. \tag{78}$$

The exact numerical solution (full line) is compared with our analytical solution (circles) from equation (63). We note that

$$S^R(E)_{ij} = \exp\left(-\mathrm{i}(d_i + d_j)\right) S(E)_{ij}. \tag{79}$$

The phases of the reduced scattering matrix vary slowly with energy compared with those of $\mathbf{S}(E)$. As it follows from equation (49), Ψ is equal to ± 1 as long as the double-passage formula is justified. Φ includes the quantum phases ϕ and ψ as well as the adiabatic phases Δ_1 and Δ_2. In figures 6 and 7 it can also be seen that the transition probability for asymptotically high energy has a simple form,

$$|S_{12}|^2 \sim \sin^2(2\theta(-\infty)) \sin^2\left(\tfrac{1}{2}\sqrt{E} \ln \frac{a_1}{a_2}\right) \tag{80}$$

as follows from equation (46) in the limit $\delta \to 0$. In figure 6 the Stueckelberg oscillations can be seen not only in the total transition probability, $P(E)$, but also in the **S**-matrix phase, $\Phi(E)$. In figure 7 these oscillations are very slow since the adiabatic potentials are almost parallel and $U_1 - U_2$ is small.

The above comparison of exact and analytical values cannot be done, strictly speaking, for the non-adiabatic transition matrix. This is because the reduced scattering matrix in the form of double passage has only two independent parameters, P and Φ,

$$\mathbf{S}^R(E) = \begin{pmatrix} \mathrm{i}\sqrt{1-P(E)}\exp(\mathrm{i}\pi\Phi(E)/2) & -\sqrt{P(E)} \\ -\sqrt{P(E)} & \mathrm{i}\sqrt{1-P(E)}\exp(-\mathrm{i}\pi\Phi(E)/2) \end{pmatrix} \tag{81}$$

which cannot provide enough equations for the three parameters of the non-adiabatic transition matrix, p, ϕ and ψ. In other words, for any non-adiabatic transition matrix **I** we can find a group of matrices $\mathbf{I}U(\omega;\ E)$,

$$\mathbf{U}(\omega;\ E) \equiv \begin{pmatrix} \pm\sqrt{1-\omega} & \mp\sqrt{\omega}\exp(-\mathrm{i}(\Delta_2 - \Delta_1)) \\ \pm\sqrt{\omega}\exp(\mathrm{i}(\Delta_2 - \Delta_1)) & \pm\sqrt{1-\omega} \end{pmatrix} \tag{82}$$

$0 < \omega < 1$, resulting in the same matrix $\mathbf{S}(E)$. There is only one phase factor in the above matrix, $\Delta_2(E) - \Delta_1(E)$, which compensates the difference of adiabatic phase shifts between the turning points and the reference point. If used in equation (63) instead of **I**, **U** yields the same scattering matrix as $\mathbf{I} = \mathbf{1}$.

6. Concluding remarks

In this work we have solved the exponential potential model by semiclassical methods. The final expressions of the **S**-matrix and the non-adiabatic transition matrix are given in terms of adiabatic potentials and the two parameters δ_1 and δ_2, which are defined by the general contour integrals and are free from particular parameters of the exponential model. The expressions for the non-adiabatic transition probability as well as the dynamical phases in terms of δ_1 and δ_2 give a new link between the attractive and repulsive case. Because δ_1 and δ_2 are generally defined by contour integrals of adiabatic momenta, the theory works well even at low energies. An interesting oscillation of the total transition probability was found at energies lower than the diabatic crossing point. This is because the adiabatic avoided-crossing point is much lower than the diabatic one. Our semiclassical treatment can reproduce even this oscillation. The present theory is expected to be applicable to a broader class of potential models which have similar singularity structures in the complex plane.

The appendices provide useful mathematical descriptions that are sufficient for understanding the results in sections 2–4.

Acknowledgments

The present research was partially supported by the International Scientific Research Programme and also by Grant-in-Aid for Scientific Research on Priority Area 'Molecular Physical Chemistry' and a Research Grant 10440179 from The Ministry of Education, Science, Sports and Culture of Japan.

Appendix A. Hankel functions

First let us clarify what kind of Bessel functions we use for the four contour integrals. On the contours asymptotically bound to the upper half of the complex p-plane the $H^{(1)}_{-\mathrm{i}\nu}(\rho p)$ function is used, while on those leading to the lower half-plane $H^{(2)}_{\mathrm{i}\nu}(\rho p)$ denotes the transformation kernel. Then the asymptotic form of the wavefunctions follows from the following expansions: for $\rho \to \infty$ ($z \to \infty$) (corresponding to the closed channel region)

$$H^{(1)}_{-\mathrm{i}\nu}(z) = \sqrt{\frac{2}{\pi z}}\mathrm{e}^{-\pi\nu/2}\exp\left(\mathrm{i}\left(z-\pi/4\right)\right) + \mathrm{O}\left(z^{-3/2}\right) \tag{A1}$$

and

$$H^{(2)}_{\mathrm{i}\nu}(z) = \sqrt{\frac{2}{\pi z}}\mathrm{e}^{-\pi\nu/2}\exp\left(-\mathrm{i}\left(z-\pi/4\right)\right) + \mathrm{O}\left(z^{-3/2}\right) \qquad (z \to \infty)$$

and for $\rho \to 0$ ($z \to 0$) (corresponding to the open channel region)

$$H^{(1)}_{-\mathrm{i}\nu}(z) = -\frac{1}{\sinh(\pi\nu)}\left(\tfrac{1}{2}z\right)^{\mathrm{i}\nu}\frac{1}{\Gamma(1+\mathrm{i}\nu)}\left(1-\frac{\left(\frac{1}{2}z\right)^2}{1+\mathrm{i}\nu}\right)\left[1+\mathrm{O}(z^2)+\mathrm{O}(\exp(-\pi\nu))\right] \tag{A2}$$

and

$$H^{(2)}_{\mathrm{i}\nu}(z) = -\frac{1}{\sinh(\pi\nu)}\left(\tfrac{1}{2}z\right)^{-\mathrm{i}\nu}\frac{1}{\Gamma(1-\mathrm{i}\nu)}\left(1-\frac{\left(\frac{1}{2}z\right)^2}{1-\mathrm{i}\nu}\right)\left[1+\mathrm{O}\left(z^2\right)+\mathrm{O}(\exp(-\pi\nu))\right].$$

In equation (A2) it is convenient to take

$$\left(1-\frac{\left(\frac{1}{2}z\right)^2}{1\pm\mathrm{i}\nu}\right) \simeq \exp\left(\frac{\mathrm{i}z^2}{4\nu}\right) \tag{A3}$$

and to make the expansion series in ν,

$$\arg\left(\Gamma(1+\mathrm{i}\nu)\right) = \tfrac{1}{4}\pi + \nu\ln\nu - \nu + \mathrm{O}(\nu^{-1}). \tag{A4}$$

Finally, we give the semiclassical Hankel functions. Substituting $Z(z) = y(z)/\sqrt{z}$ in equation (11) we obtain the WKB form of $y(z)$. Since $\nu^2 \gg 1$, the two independent solutions read

$$H^{(1,2)}_{\mp\mathrm{i}\nu}(z) \sim \frac{1}{\sqrt{\nu^2+z^2}}\exp\left(\pm\mathrm{i}\int^z\sqrt{1+\frac{\nu^2}{\xi^2}}\,\mathrm{d}\xi\right). \tag{A5}$$

Appendix B. Local solutions of equation (15)

Here we give the mathematical preliminaries of evaluating wavefunctions at $\rho \to \infty$, i.e. the solution in the classically inaccessible region. We expand equation (15) at each singular point of its solution (cf equation (13)), because all smoothly varying terms are effectively cancelled by the highly oscillating transforming Hankel functions in equation (10). After finding the local solutions we match them to the asymptotic WKB form.

Let us start with Whittaker's standard form of confluent hypergeometric equation, i.e. in our case

$$\frac{\mathrm{d}^2}{\mathrm{d}z^2}f(z) + \left(-\frac{1}{4}+\mathrm{i}\frac{\Delta}{z}\right)f(z) = 0 \qquad \mathrm{Im}\,\Delta = 0. \tag{B1}$$

The independent solutions of (B1) are given in terms of confluent hypergeometric functions Φ and Ψ as

$$f_1(z) = z\exp(-z/2)\Phi(1-\mathrm{i}\Delta, 2, z) \tag{B2}$$

and

$$f_2(z) = z\exp(-z/2)\Psi(1-\mathrm{i}\Delta, 2, z).$$

Taylor series to the order $\mathrm{O}(1/|z|)$ yield

$$f_1(z) \simeq z^{\mathrm{i}\Delta}\frac{\exp(-z/2)\exp(\mathrm{i}\pi\epsilon)^{1-\mathrm{i}\Delta}}{\Gamma(1+\mathrm{i}\Delta)} - z^{-\mathrm{i}\Delta}\frac{\exp(z/2)}{\Gamma(1-\mathrm{i}\Delta)} \tag{B3}$$

and

$$f_2(z) \simeq z^{\mathrm{i}\Delta}\exp(-z/2) \qquad \epsilon \equiv \mathrm{sgn}(\mathrm{Im}\, z) \qquad \exp(z) \simeq 1$$

with the last relation indicating that p is still sufficiently close to the point of expansion. To match (B3) directly to the WKB solutions of non-expanded Schrödinger equation we need to introduce

$$f_+(z) \equiv f_2(z) \simeq z^{\mathrm{i}\Delta} \tag{B4}$$

and

$$f_-(z) \equiv Qf_1(z) + Rf_2(z) \simeq z^{-\mathrm{i}\Delta}$$

where

$$R = \frac{\Gamma(-\mathrm{i}\Delta)}{\mathrm{i}\Delta}\exp(\mathrm{i}\pi\epsilon)^{1-\mathrm{i}\Delta}. \tag{B5}$$

Close to the origin it holds

$$\Phi(1-\mathrm{i}\Delta, 2, z) \simeq 1 + \mathrm{o}(z) \qquad \text{and} \qquad \Psi(1-\mathrm{i}\Delta, 2, z) = \frac{1}{\Gamma(1-\mathrm{i}\Delta)}\frac{1}{z} + \mathrm{o}(\ln(z)). \tag{B6}$$

Thus only the z^{-1} singular term arising from Ψ contributes $2\pi\mathrm{i}$ (and the respective multiplicative constants) to the integral of the type

$$\int \frac{\mathrm{d}z}{z} f_\pm(z)H(\kappa z) \qquad \kappa \to \infty. \tag{B7}$$

Appendix C. Confluent hypergeometric integral formulae

The confluent hypergeometric function Ψ which appears in equation (B1) is defined as,

$$\Psi(a, c, \xi) = \frac{1}{2\pi\mathrm{i}}\exp(-a\pi\mathrm{i})\Gamma(1-a)\int_{\infty\mathrm{e}^{\mathrm{i}\phi}}^{0^+} \mathrm{e}^{-\xi t}t^{a-1}(1+t)^{c-a-1}. \tag{C1}$$

Φ is related to Ψ by the Kummer relation

$$\Psi(a, c, \xi) = \frac{\Gamma(c-1)}{\Gamma(a-c+1)}\Phi(a, c, \xi) + \frac{\Gamma(c-1)}{\Gamma(a)}\xi^{1-c}\Phi(a-c+1, 2-c, \xi) \tag{C2}$$

and we have

$$\Phi(a, c, \xi) = 1 + \mathrm{o}(\xi). \tag{C3}$$

Appendix D. Bessel–Fourier contour integrals at $x \to -\infty$

Equation (15) cannot be solved in the WKB form when $x \to -\infty$, since the saddle points approach the singularities $p = \pm\sqrt{|a_i|}$. That is why we expand equation (15) to series, solve it locally for $p \sim \sqrt{a_i}$ and match to the asymptotic WKB form. From now on we assume that the definition of $\sqrt{a_i}$ or $\sqrt{c_i}$ is chosen for each contour in accordance with the respective branch cut (see figure 1). Substituting

$$z_i = -\frac{2\mathrm{i}\mu}{\sqrt{a_i}}(p - \sqrt{a_i}) \tag{D1}$$

we obtain (with the accuracy up to $\mathrm{O}(\delta_i)$, $\mathrm{O}(z_i)$)

$$\frac{\mathrm{d}^2 f_1}{\mathrm{d}z_i^2} + \left(-\frac{1}{4} + \mathrm{i}\frac{\delta_i}{z_i}\right) f_1 = 0. \tag{D2}$$

The asymptotic form of solutions of local equation (D2) (see equation (B4)) corresponds to that of the WKB solutions in equation (19). Thus they can be matched. Making use of equations (12), (A1) and (B1)–(B7) we finally obtain

$$I^{(1)}_{mn}(\rho) = \frac{\pi}{\sqrt{\mu}} \frac{s_n}{\delta_m \Gamma(\mathrm{i}s_n\delta_m)} (a_m - a_{3-m})^{\mathrm{i}s_n\delta_m} |a_m|^{\mathrm{i}\nu/2} \left|\frac{a_m}{\mu}\right|^{\mathrm{i}s_n\delta_m} \mathrm{e}^{(\frac{1}{2}\pi(-\nu+\delta_m))}$$
$$\times \frac{\exp\left(|\sqrt{a_m}|\rho - \pi\nu/2\right)\sqrt{2}}{\left(\pi|\sqrt{a_m}|\rho\right)^{1/2}} \qquad c_m \equiv (-1)^{m-1} \quad \rho \to \infty. \tag{D3}$$

Since only the singularity contributes to the integral, from equation (12) it follows that

$$I^{(2)}_{mn}(\rho) = (\beta_1 - a_m)\, I^{(1)}_{mn}(\rho) \qquad \rho \to \infty. \tag{D4}$$

Thus the adiabatic wavefunctions are obtained by rotating the diabatic ones

$$\phi_1(\rho \to \infty) = (\gamma_{11} I^{(1)}_{11} + \gamma_{12} I^{(1)}_{12})(\cos\theta_0 - (\beta_1 - a_1)\sin\theta_0)$$
$$+(\gamma_{21} I^{(1)}_{21} + \gamma_{22} I^{(1)}_{22})(\cos\theta_0 - (\beta_1 - a_2)\sin\theta_0) \tag{D5}$$

and

$$\phi_2(\rho \to \infty) = (\gamma_{11} I^{(1)}_{11} + \gamma_{12} I^{(1)}_{12})(\sin\theta_0 + (\beta_1 - a_1)\cos\theta_0)$$
$$+(\gamma_{21} I^{(1)}_{21} + \gamma_{22} I^{(1)}_{22})(\sin\theta_0 + (\beta_1 - a_2)\cos\theta_0)$$

where

$$\theta_0 \equiv \lim_{x\to-\infty} \theta(x).$$

It can be seen easily that

$$\cos\theta_0 - (\beta_1 - a_1)\sin\theta_0 \equiv 0 \equiv \sin\theta_0 + (\beta_1 - a_2)\cos\theta_0 \tag{D6}$$

while the other terms in equation (D5) are non-vanishing and growing exponentially with ρ. Since the adiabatic wavefunctions should vanish when $x \to -\infty$, we obtain the two conditions

$$\gamma_{21} I^{(1)}_{21} + \gamma_{22} I^{(1)}_{22} = 0 \qquad \text{and} \qquad \gamma_{11} I^{(1)}_{11} + \gamma_{12} I^{(1)}_{12} = 0. \tag{D7}$$

Appendix E. Bessel–Fourier contour integrals at $x \to \infty$

The WKB solution (19) of the Schrödinger equation (15) in the approximation (20) has the form (cf equations (13) and (19))

$$F_1^{(n)}(p) = \frac{1}{\sqrt{\mu}} \left(p^2 - a_1\right)^{\mp i\delta_1 - 1} \left(p^2 - a_2\right)^{\mp i\delta_2 - 1} \qquad n = 1, 2. \tag{E1}$$

Making use of the Bessel function expansions (cf equations (A2) and (A4)) we obtain

$$I_{mn}^{(1)}(\rho \to 0) = \frac{\rho^{ic_n \nu}}{\sqrt{\mu}} e^{ic_n(\pi/4 - \phi_0)} \int_{C_{mn}} (p^2 - a_1)^{\mp i\delta_1 - 1} (p^2 - a_2)^{\mp i\delta_2 - 1} p \, dp. \tag{E2}$$

This integral can be reduced to the confluent hypergeometric function integral of equation (C1) by means of the substitution

$$t_m = \frac{p^2 - a_m}{a_{3-m} - a_m}. \tag{E3}$$

Evaluating the confluent hypergeometric functions at zero argument (see equations (C2) and (C3)) we obtain

$$I_{mn}^{(1)}(\rho \to 0) = -\pi c_m \frac{\rho^{ic_n \nu}}{\sqrt{\mu}} e^{ic_n(\phi_0 + \pi/4)} \frac{\Gamma(1 + ic_n\delta)(a_2 - a_1)^{-ic_n\delta - 1}}{\Gamma(1 + ic_n\delta_1)\Gamma(1 + ic_n\delta_2)}. \tag{E4}$$

When evaluating $I_{mn}^{(2)}$, the integrand in equation (E2) differs only by

$$\beta_1 - p^2 = c_m(a_2 - a_1)(t_m + \delta_m/\delta). \tag{E5}$$

Thus in the case of ψ_2 the leading-order terms coming from equation (C2) cancel. This is the reason why the ρ^2 term of equation (A3) must be retained here. It comes from equations (A2), (A3), (C1), (C2), and gives the difference between $\rho^{i\nu}$ and $\rho^{i\mu}$. The final result is

$$I_{mn}^{(2)}(\rho \to 0) = -c_n \frac{\rho^{ic_n \mu}}{\sqrt{\mu}} e^{ic_n(\phi_0 - \delta \ln(4\nu) - \pi/4)} e^{\pi\delta/2} \Gamma(-ic_n\delta) e^{-\pi\delta_m} \operatorname{sh}(\pi\delta_m). \tag{E6}$$

Appendix F. Proof of the unitarity of S-matrix

Using the following identities:

$$\Gamma(1 - i\delta) = -i\delta\Gamma(-i\delta) \tag{F1}$$

$$|\Gamma(i\delta)|^2 = \frac{\pi}{\delta \operatorname{sh}(\pi\delta)} \tag{F2}$$

and

$$(a_2 - a_1) = \frac{\delta}{\sqrt{\delta_1\delta_2}} \tag{F3}$$

we can find that the **S**-matrix in equations (44*a*)–(44*d*) satisfies

$$S_{12} = S_{21} \qquad |S_{11}|^2 = |S_{22}|^2 \qquad \text{and} \qquad |S_{11}|^2 + |S_{12}|^2 = 1. \tag{F4}$$

The last unitarity condition to be proven is

$$S_{11}S_{12}^* + S_{12}S_{22}^* = 0 \tag{F5}$$

or in other words

$$\arg(S_{11}) + \arg(S_{22}) - 2\arg(S_{12}) = (2k+1)\pi \qquad k \in Z. \tag{F6}$$

Taking into account the extracted prefactors in the **S**-matrix of equations (44*a*)–(44*d*) it is sufficient to prove that

$$\begin{aligned}\arg\left[\mathrm{sh}(\pi\delta_1)\,\mathrm{e}^{\mathrm{i}\alpha_1} + \mathrm{sh}(\pi\delta_2)\,\mathrm{e}^{\pi\delta}\mathrm{e}^{\mathrm{i}\alpha_2}\right] + \arg\left[\mathrm{sh}(\pi\delta_1)\,\mathrm{e}^{\mathrm{i}\alpha_2} + \mathrm{sh}(\pi\delta_2)\,\mathrm{e}^{\pi\delta}\mathrm{e}^{\mathrm{i}\alpha_1}\right] \\ = 2\arg\left[\mathrm{e}^{\mathrm{i}\alpha_2} - \mathrm{e}^{\mathrm{i}\alpha_1}\right] + (2k+1)\pi\end{aligned} \tag{F7}$$

which is just an algebra.

Appendix G. Adiabatic scattering phase shifts

First we give an account of real definite integrals

$$\begin{aligned}\int_\epsilon^x \frac{\mathrm{d}x}{x-d}\sqrt{\frac{x-\epsilon}{x}} &= \ln|x-d| - \ln|d| + \frac{\epsilon}{2d}(1 - \ln|\epsilon| - \ln|x-d| \\ &\quad + \ln|d| + \ln|x| + 2\ln 2) + \mathrm{O}(\epsilon^2)\end{aligned} \tag{G1}$$

$$\int_\epsilon^x \frac{\mathrm{d}x}{(x-d)(x-e)}\sqrt{\frac{x-\epsilon}{x}} = \frac{1}{e-d}(\ln|d| - \ln|x-d| - \ln|e| + \ln|x-e|) + \mathrm{O}(\epsilon) \tag{G2}$$

and

$$\int_{\mathrm{i}\nu}^x \sqrt{1 + \frac{\nu^2}{\xi^2}}\,\mathrm{d}\xi = \nu + \frac{\nu}{2}\ln\frac{x}{\nu} + \frac{x^2}{4\nu} + \mathrm{O}(\nu^{-3/2}). \tag{G3}$$

Manipulating the second term in equation (55) yields (note that $c_i < 0$)

$$\int_{\sqrt{c_i}}^p \sqrt{\frac{(p^2-c_1)(p^2-c_2)}{(p^2-a_1)(p^2-a_2)}}\frac{\mathrm{d}p}{p} = \tfrac{1}{2}\int_{c_i-a_i}^{p^2-a_i} \frac{\mathrm{d}x}{x+a_i}\sqrt{\frac{x-(c_i-a_i)}{x}}\sqrt{1 - \frac{c_{3-i} - a_{3-i}}{x-(a_{3-i}-a_i)}}. \tag{G4}$$

Evaluating the phase shifts d_i and Δ_i we can expand the second square root in equation (G4) with respect to $a_i - c_i$, which is proportional to the inverse of energy. Using identities in equations (G1)–(G3), we can evaluate all the phase shifts. The results are given in equations (56)–(58). The last term in equation (58) originates from the following:

$$\Delta_1 - \Delta_2 = \mathrm{Re}\left\{\int_{x_1^t}^{x_*} k_1(x)\,\mathrm{d}x - \int_{x_2^t}^{x_*} k_2(x)\,\mathrm{d}x - \int_{x_*}^{\mathrm{Re}\,x_*}(k_1(x)+k_2(x))\,\mathrm{d}x\right\}. \tag{G5}$$

The first two integrals in equation (G5) follow from equations (G1)–(G3), while the last one can be evaluated by Taylor expansion,

$$k_j(x) = \sqrt{E - u_j^a(x)} \simeq \sqrt{E} - \frac{u_j^a(x)}{2\sqrt{E}} \tag{G6}$$

since the last integration path is separated from the turning point. Then the exact result is the same as in the attractive case [14], i.e.

$$\frac{1}{2\sqrt{E}}\,\mathrm{Re}\left\{\int_{\mathrm{Re}\,x_c}^{x_c}(u_1^a(x) - u_2^a(x))\,\mathrm{d}x\right\} = 2\sqrt{\delta\delta_2} + \delta_1\ln\frac{\sqrt{\delta}-\sqrt{\delta_2}}{\sqrt{\delta}+\sqrt{\delta_2}}. \tag{G7}$$

Appendix H. Contour integrals to define δ_j

The parameters δ_1 and δ_2 introduced in equation (21) are defined as [14]

$$\delta_j = \frac{1}{2\pi \mathrm{i}} \oint_{L_j} \sqrt{P_0}\, \mathrm{d}p \tag{H1}$$

where the L_jth contour encircles the branch cut between $\sqrt{a_j}$ and $\sqrt{c_j}$ in the positive direction. For details see figure 2. Equation (21) is a result of the high-energy limit of equation (H1), when we expand $\sqrt{P_0}$ in terms proportional to $a_j - c_j$. Let us show now that equation (H1) can be put into the form of an adiabatic momentum contour integral. We start with equations (22) and (25) and the easier attractive case. Then it suffices to find contours in the ρ^2-plane corresponding to the contours L_j in the p-plane (using equation (24)),

$$\rho^2 = P_0(p_j^{\dagger}) - \frac{\nu^2}{p_j^{\dagger 2}}. \tag{H2}$$

The transformed contours are shown in figure 3. None of these closed contours encircles $\rho^2 = 0$ or ρ_0^2, the solution of

$$p_j^{\dagger}(\rho_0) = 0 \tag{H3}$$

given by

$$\rho_0^2 = -\frac{4\beta_1(U_1 - U_2)}{\beta_1\beta_2 - 1} \qquad (j = 1, (2) \text{ attractive (repulsive) case}) \tag{H4}$$

that is why the last integral in equation (22) on such a contour must vanish,

$$\oint \sqrt{1 + \frac{\nu^2}{\xi^2}}\, \mathrm{d}\xi \equiv 0. \tag{H5}$$

Since the contours L_i in the ρ^2-plane are symmetric with respect to the real axis and the integrand in equation (H1) is the complex conjugate with respect to this axis, the real part of the integral must vanish and the contribution of the imaginary part coming from the upper and lower half-plane doubles. Then equations (65) and (66) follow from figure 3 and equations (22) and (H5). Note that the integration path in the x-plane is just distorted in a way which does not change the result (see figures 3 and 4).

Though in the repulsive case the contours for δ_1 and δ_2 in the p-plane (see figure 2) are very similar to those in the attractive case, the general expressions in terms of contour integrals in the x-plane are quite different. Let us start with a note on the difference between the two cases,

$$V_i \to -V_i \qquad \beta_i \to -\beta_i \qquad a_i \to -a_{3-i} \qquad \text{and} \qquad c_i \to -c_{3-i}. \tag{H6}$$

As a result,

$$\delta_i \to \delta_{3-i} \tag{H7}$$

both for the approximate expression of δ_i from equation (21) and the exact one from equations (16) and (H1). The change of the sign in equation (H6) is equivalent to

$$x \to x \pm \mathrm{i}\pi \tag{H8}$$

leaving the pre-exponential constants V_i $(i = 1, 2)$ unchanged.

The contours for δ_1 and δ_2 in the ρ^2-plane (repulsive case) are shown in figure 5. Both of them encircle zero, thus before they can be moved through it, the behaviour of the integrand at this point must be clarified. We have

$$\sqrt{P_0(p_j)}\,\frac{\mathrm{d}p_j}{\mathrm{d}(\rho^2)} = (-1)^j\,\frac{\nu^2-\mu^2}{4p_j^2\rho^4}\,\frac{p_{3-j}^2-\beta_2}{\sqrt{1+\left((\beta_1-\beta_2)/2-(\mu^2-\nu^2)/2\rho^2\right)^2}}\sqrt{zp^2+\nu^2}. \tag{H9}$$

From the above equations it follows that

$$\sqrt{P_0(p_1)}\,\frac{\mathrm{d}p_1}{\mathrm{d}(\rho^2)} = C + \mathrm{O}(\rho^2) \qquad C \in Z \tag{H10}$$

and

$$\sqrt{P_0(p_2)}\,\frac{\mathrm{d}p_2}{\mathrm{d}(\rho^2)} = -\frac{\mu}{2z} + \mathrm{O}(1). \tag{H11}$$

As a result of equation (H11) the zero has a contribution to δ_2,

$$\frac{1}{2\pi\mathrm{i}}\oint_0 \sqrt{P_0(p_2)}\,\frac{\mathrm{d}p_2}{\mathrm{d}(\rho^2)}\,\mathrm{d}\rho^2 = \frac{\mu}{2}. \tag{H12}$$

While the contour for δ_1 avoids ρ_0^2 (the contour L_1 in the p-plane can go around $\sqrt{\beta_1}$ instead of the turning point $\sqrt{c_1}$), the contour for δ_2 does not (the contour L_2 in the p-plane can go around $p=0$ which corresponds to ρ_0^2). That is why there is one more contribution to δ_2 from the integral in the complex $\rho p(\rho)$-plane,

$$\frac{1}{2\pi\mathrm{i}}\oint_{\rho_0 p_1(\rho_0)}\sqrt{1+\frac{\nu^2}{\xi^2}}\,\mathrm{d}\xi = -\frac{\nu}{2}. \tag{H13}$$

The contributions to δ_2 arising from the zero $\rho^2=0$ and from the second term in equation (22) finally give

$$\delta = \delta_1 + \delta_2 = \tfrac{1}{2}(\mu-\nu). \tag{H14}$$

The contour integrals encircling the complex crossing points in the ρ^2-plane both for δ_1 and δ_2 have the form of equation (66), differing just by a sign due to the opposite fixing of branch cuts (in figure 5(a)) the integrand is k_1, while in figure 5(b) the integrand is k_2).

The alternative way to examine the contours is as follows. We start with equations (22) and (25) which can be modified to give the following form:

$$\oint_{L_j} P_0(p)\,\mathrm{d}p = \oint \sqrt{E-u_j^{(a)}(\rho^2)}\,\frac{\mathrm{d}(\rho^2)}{\rho^2} - \frac{\nu}{2}\left[\ln\frac{1+2\sqrt{E-u_j^{(a)}}}{1-2\sqrt{E-u_j^{(a)}}}\right]. \tag{H15}$$

The closed contours are always oriented in the positive direction and encircle zero in the ρ^2-plane. Evaluating the second integral in equation (H15) by the residue theorem and taking into account that $[\ ] = 2\mathrm{i}\pi$ we obtain the same results as above.

References

[1] Nikitin E E and Umanskii S Ya 1984 *Theory of Slow Atomic Collisions* (Berlin: Springer)
[2] Medvedev E S and Osherov V I 1994 *Radiationless Transitions in Polyatomic Molecules (Springer Series in Chemical Physics vol 57)* (Berlin: Springer)
[3] Nakamura H 1991 *Int. Rev. Phys. Chem.* **10** 123
[4] Joye A and Pfister C E 1999 Exponential estimates in adiabatic quantum evolution *12th Int. Congress of Mathematical Physics: ICMP '97* ed D D Wit, A J Bracken, M D Gould and P A Pearce (Cambridge: International Press)
[5] Zhu C and Nakamura H 1992 *J. Math. Phys.* **33** 2697
[6] Nakamura H and Zhu C 1996 *Commun. At. Mol. Phys.* **32** 249
[7] Nakamura H 1996 Nonadiabatic transitions: beyond Born–Oppenheimer *Dynamics of Molecules and Chemical Reactions* ed R E Wyatt and J Z H Zhang (New York: Dekker) ch 12
[8] Zhu C and Nakamura H 1998 *J. Chem. Phys.* **109** 4689
[9] Zhu C and Nakamura H 1996 *Chem. Phys. Lett.* **258** 342
Zhu C and Nakamura H 1997 *Chem. Phys. Lett.* **274** 205
[10] Zhu C and Nakamura H 1997 *J. Chem. Phys.* **106** 2599
Zhu C and Nakamura H 1997 *J. Chem. Phys.* **107** 7839
Zhu C and Nakamura H 1998 *J. Chem. Phys.* **108** 7501 (erratum)
[11] Osherov V I and Voronin A I 1994 *Phys. Rev.* A **49** 265
[12] Osherov V I and Nakamura H 1996 *J. Chem. Phys.* **105** 2770
[13] Osherov V I and Nakamura H 1999 *Phys. Rev.* A **59** 2486
[14] Osherov V I, Ushakov V G and Nakamura H 1998 *Phys. Rev.* A **57** 2672
[15] Abramowitz M and Stegun I 1972 *Handbook of Mathematical Functions* (New York: Dover)
[16] Joye A, Milleti G and Pfister C E 1991 *Phys. Rev.* A **44** 4280